Seismic deformation demands on rectangular structural walls in frame-wall systems

İlker Kazaz[*]

Department of Civil Engineering, Erzurum Technical University, 25050 Erzurum, Turkey

Abstract. A parametric study was conducted to investigate the seismic deformation demands in terms of drift ratio, plastic base rotation and compression strain on rectangular wall members in frame-wall systems. The wall index defined as ratio of total wall area to the floor plan area was kept as variable in frame-wall models and its relation with the seismic demand at the base of the wall was investigated. The wall indexes of analyzed models are in the range of 0.2-2%. 4, 8 and 12-story frame-wall models were created. The seismic behavior of frame-wall models were calculated using nonlinear time-history analysis and design spectrum matched ground motion set. Analyses results revealed that the increased wall index led to significant reduction in the top and inter-story displacement demands especially for 4-story models. The calculated average inter-story drift decreased from 1.5% to 0.5% for 4-story models. The average drift ratio in 8- and 12-story models has changed from approximately 1.5% to 0.75%. As the wall index increases, the dispersion in the calculated drifts due to ground motion variability decreased considerably. This is mainly due to increase in the lateral stiffness of models that leads their fundamental period of vibration to fall into zone of the response spectra that has smaller dispersion for scaled ground motion data set. When walls were assessed according to plastic rotation limits defined in ASCE/SEI 41, it was seen that the walls in frame-wall systems with low wall index in the range of 0.2-0.6% could seldom survive the design earthquake without major damage. Concrete compressive strains calculated in all frame-wall structures were much higher than the limit allowed for design, ε_c=0.0035, so confinement is required at the boundaries. For rectangular walls above the wall index value of 1.0% nearly all walls assure at least life safety (LS) performance criteria. It is proposed that in the design of dual systems where frames and walls are connected by link and transverse beams, the minimum value of wall index should be greater than 0.6%, in order to prevent excessive damage to wall members.

Keywords: dual system; compression strain; plastic rotation; performance criteria; wall index

1. Introduction

Low-to-midrise reinforced concrete moment resisting frame buildings compose large portion of the building inventory in Turkey (Ozmen *et al*. 2013). After the M7.4 Kocaeli earthquake use of shear walls in combination with reinforced concrete moment resisting frames has gained a boost. These buildings are mostly constructed with 4-12 stories in regions of high seismicity and used for

*Corresponding author, Associate Professor, E-mail: ilkerkazaz@erzurum.edu.tr

residential accommodation. Dual systems are preferred in earthquake resistant design, because the interaction of these two distinct structural forms enables the control of drifts in the building due to their inherent characteristics. Different behavior modes arise during this interaction. The failure mechanism of the wall not only depends on the geometry of the cross section, but also on the way the wall is loaded. If the wall is subjected to a large moment which produces yielding with low shear, the mechanism will be completely different than if loaded with low moment but large shear. The way the wall undergoes inelastic deformations will determine the path of force redistribution, and entirely dominate the subsequent response of the building (Charney and Bertero 1982).

In frame-wall systems relative rigidity of frames and walls has significant effect on deformation and strength characteristics of structural walls (Vallenas *et al*. 1979, Kayal 1986). Frame wall-interaction poses a serious problem for reinforced concrete structural walls especially in situations where the frame part of the structural system becomes stiffer as compared to the walls. Kayal (1986) investigated the effect of wall-column stiffness ratio, which is defined as the ratio of the flexural rigidities of the shear wall and the column (EI_w/EI_c), along with additional parameters such as the ratio of beam and column stiffness, load ratio (lateral to vertical load). One of the significant conclusions emerged from this study is that nonlinear idealization of the flexural characteristics of shear walls became more pronounced when shear walls are located in stiff frames since the actual characteristic of shear walls, which is "shear behavior" has to be activated.

Frame-wall structures can be composed of either structures with walls and frames connected by floor slabs, or structures with link-beams extending from frames directly to the ends of the walls. In the latter, the shear and moment transferred from beams can significantly change the moment profile causing a reduction in the inflection height of the wall. Although walls are stiff elements and has a limiting effect on the deformations when elastic action is considered, in the inelastic range after plastic hinge formation at the base of the wall, system behavior changes completely to lead to significant deformation demands. This may have profound effects on the behavior of dual systems (Lu 2002, Lazzali 2013). Because of the rigid-body displacement of such walls, rotations along the height of the wall, of the same order as that at the foundation, will be introduced at every level. Lu (2002) experimentally investigated the behavior of a six-story three-bay RC frame-wall structure with comparison to a bare ductile frame by means of earthquake simulation tests. Despite a superior performance over the ductile frame under low to moderate seismic actions, the frame-wall structure deteriorated more rapidly than the bare frame during advanced inelastic response. The advantage of a good drift control with the wall-frame system tended to diminish with the increase of inelastic deformation. This phenomenon was primarily attributed to the rocking of the wall and the associated uplift mechanism which involved highly localized inelastic deformation at the wall base region, and the amplified rotation demands on beams framing into the wall.

It is known that the performance of RC structural walls in recent earthquakes has exposed some problems with the existing design of RC structural walls. Based on section analysis and pushover analysis, Dashti *et al*. (2014) compared the nonlinear responses of the walls in terms of their lateral load capacity and curvature as well as displacement ductilities, and the effect of the code limitations on nonlinear responses of the different walls were evaluated. Behavior of shear walls is also very important for retrofit of existing buildings. Even though some recent methods are present for retrofit of existing deficient buildings (Lalaj *et al*. 2015, Özdemir and Bayhan 2015) the most common one is still adding shear walls to bare frame structures as a system level retrofit solution (Inel *et al*. 2008). The total amount and individual dimensions of added walls is the key parameter of the design stage. This paper directly addresses this issue and may be useful for designers by the provided numerical figures.

In this paper, a detailed parametric study was conducted to investigate the seismic deformation demands in terms of drift ratio, plastic base rotation and compressive strain at the base of walls in frame-wall systems. The calculated seismic demand measures were compared with available and code performance limits proposed for structural walls (ASCE 41-06 2006, Kazaz *et al.* 2012).

2. Method of analysis

The elastic and inelastic behavior and the failure mechanism of reinforced concrete frame-wall systems (dual systems) were investigated by different researchers in an approximate manner by replacing the structure with a system of idealized mechanical models (Khan and Sbarounis 1964, Heidebrecht and Stafford Smith 1973, Emori and Schnobrich 1981, Kazaz and Gülkan 2012a, Takabatake 2013). Similar to isolated cantilever wall models used in the analyses of shear wall buildings (Sözen 1989, Wallace and Moehle 1992), a simple yet effective analysis model was developed for parametric investigation of the frame-wall dual systems in this study. The purpose is to analyze a particular wall in isolated form as in the case of cantilever wall models, yet including the interaction effects in dual systems.

2.1 Frame-Wall Model: Shear-flexure beam formulation

The continuum method utilizing combined shear-flexure beam formulation for the analysis of frame-wall and coupled wall systems was used for the derivation of characteristic relations. The method involves the floor by floor interaction of planar panels consisting of walls, or frames, or both. The lateral loading is usually distributed between the component structures in proportion to their rigidities at each story. The method is widely used to calculate the dynamic properties of tall buildings and used in studies that deal with the behavior of variety of structures. The method can be easily programmed allowing a reduction in the idealization effort without going through detailed structural modeling by representing each structure with only one parameter (Kazaz and Gülkan 2012a).

A design procedure that depends on a new shear-flexure beam continuum formulation of frame-wall structures (Kazaz and Gülkan 2012a) was used to quantify the seismic shear force distribution among the wall and frame components of frame-wall models and to calculate the amount of flexural reinforcement at the boundary elements of the walls. The formula for the lateral deflection of the frame-wall structure (combined shear-flexure beam) reads as

$$\frac{d^4y}{dx^4} - \alpha^2 \frac{d^2y}{dx^2} = \frac{w(x)}{EI_w} \qquad \text{where} \qquad \alpha^2 = \frac{GA + \eta}{EI_w} \tag{1}$$

In this equation GA is the equivalent story shear rigidity of the frame component and EI_w is the flexural rigidity of shear wall members, η holds for the equivalent flexural rigidity of beams framing to wall. Last term especially increases the accuracy of the calculations when the transverse beams have substantial flexural capacity so increase the flexural resistance of the wall providing a constraint on the wall rocking by the reactions from transverse beams in cases where the uplift due to rocking is significant. Another improvement in Kazaz and Gülkan's (2012a) formulation is the correction for the shear force boundary condition at the base of the wall for which the frame shear is no more zero at the base in regards to classical formulation. The continuum formulation was

verified against 3D frame-wall finite element model results and displayed very good match for all response quantities.

The main parameter that determines the dominant deformation mode of a shear-flexure beam is the parameter αH, where H is the building height. The deflected shape of structures composed of structural walls as lateral load resisting system can be approximated by using values of αH between 0 and 2. The deflected shape of dual systems or braced systems can be calculated by values of αH typically between 1.5 and 6. For buildings composed of only moment-resisting frames the values of αH between 5 and 20 can be used (Miranda and Reyes 2002).

Comprehensive descriptions, assumptions, derivations and case studies of the continuum formulation can be found in Kazaz and Gülkan (2012a), solving the differential equation in Eq. (1) only the final expressions for the bending moment and shear force at the base of wall component under triangular distribution of lateral loads are given below. These equations facilitate the design of models used in the parametric study. The bending moment at the base of the wall can be calculated using the following expression

$$M_w = \frac{\dfrac{V_t \sinh(\alpha H_1)}{\alpha} - \dfrac{V_t h_{cc}^4}{3EI_c f}\left[\dfrac{\alpha h_{cc} \sinh(\alpha H_1)}{2} + \cosh(\alpha H_1)\right] - \dfrac{w_1}{\alpha^3 H}\left[\alpha h_{cc} \cosh(\alpha H_1) + \sinh(\alpha H_1) - \alpha H\right]}{\left(1 - \dfrac{h_{cc}^3}{4EI_w f}\right)\alpha h_{cc} \sinh(\alpha H_1) + \left(1 - \dfrac{h_{cc}^3}{2EI_w f}\right)\cosh(\alpha H_1)} \tag{2}$$

in which V_t=total seismic base shear, h_{cc}=contra-flexure height on the columns at the base story taken as 70% of the story height, H=total building height, $H_1=H-h_{cc}$, EI_w=total flexural rigidity of walls. The flexibility factor for the base story f is calculated as

$$f = \frac{h_{cc}^3}{6EI_w} - \frac{h_{cc}^3}{3EI_c} - \frac{h_{cc}}{GA_w} \tag{3}$$

In this equation EI_c is the total flexural rigidity of all columns in the base story, GA_w is the total shear rigidity of the walls. The amplitude of triangularly distributed lateral load is $w_1 = 2V_t H/(H^2 - h_{cc}^2)$. The base shear force on the wall component can be calculated using

$$V_w = M_w \frac{h_{cc}^2}{2fEI_w} - V_t \frac{h_{cc}^3}{3fEI_c} \tag{4}$$

When multiple shear walls exist in the system the calculated wall component bending moment and shear force are distributed according to flexural rigidities of each wall.

2.2 Prototype structure used to derive model parameters

Using different combinations of wall length, wall number and configuration in the plan as shown in Fig. 1(a) and increasing the building height, various dual structures, where frames and walls interacting at different levels, were obtained. Primary interest in such an arrangement was to quantify the degree of frame-wall interaction and the amount of walls in the system with representative generalized parameters to investigate their effects on the response of structural walls. Then using relations derived for the static and dynamic properties of these systems, single wall-equivalent frame models that depend mainly on a specific wall length and a wall index was developed.

(a) Bare Frame   (b) Frame-wall
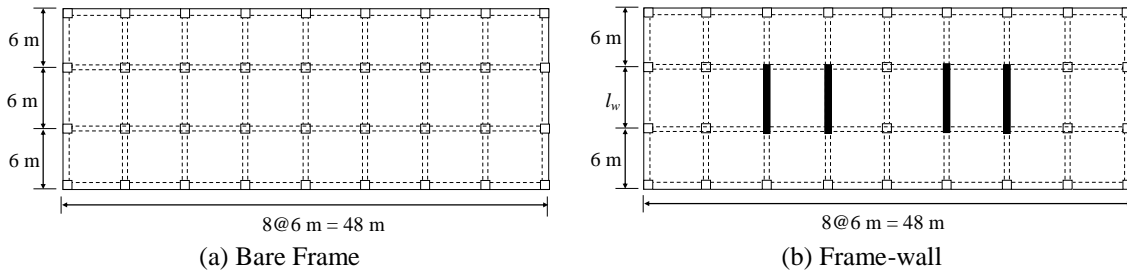
Fig. 1 Plan view of frame-wall configurations (number and length of walls are variable)

The general plan configuration shown in Fig. 1(a) was used as the base model for all the prototype frame-wall structures. The structure is composed of nine 3-span frames in the transverse direction and four 8-span frames in the longitudinal direction. For the parametric analyses wall length (L_w), building-wall height (H_w) and wall index-p calculated as the ratio of the total wall area to the floor plan area (A_w/A_f) in one direction was used as variables. By increasing the number of walls in the central bay in the transverse direction and the building height, different frame-wall arrangements are obtained as shown in Fig. 1(b). 3, 5 and 8 m long shear walls were placed in different numbers into the central bay in the transverse direction. The building heights that were considered to determine the aspect ratio of the shear walls consist of 4, 8 and 12-story structures. The 3 m inter-story height was considered to be constant along the height of the building. For the frame part the dimensions of the columns were taken as 0.6×0.6 m and the beams as 0.4×0.6 m for all models. Robust beam and column elements were used to ensure that the desired frame-wall interaction develops effectively. The behavior of each of these structures was characterized with αH parameter.

For the frame configuration given in Fig. 1, the typical values of αH were calculated and plotted against the wall index p in Fig. 2. The cracked member stiffness values were used in the calculations. The uncracked section stiffness was reduced by factor of 0.4, 0.5 and 0.5 for beams, columns and walls, respectively. αH values in the graphs are related to number of walls in the system, where in descending order each value on a curve corresponds to the structural systems with 1, 2, 3, 4, 5, 6 and 8 walls for 3 m and 5 m long walls, and 1, 2, 3, 4, 5, 6, 7 and 9 walls for 8 m walls. The same base curve in the form of $N.c.p^b$ can be used to define relation between the wall index and behavior factor, where N is the number of stories. For particular wall length and plan configuration coefficients b and c are constant regardless of the building-wall height.

Although αH is a very effective parameter in defining dynamic and static characteristics of structures, wall index-p is preferred to characterize the models since it is simpler and widely recognized parameter (Sözen 1989, Wallace and Moehle 1992). For instance Wallace and Moehle (1992) stated that typical U.S. construction for concrete buildings 5 to 20-stories tall relies on frames or combined frame-wall systems to resist lateral loads. Where walls are used, the ratio of wall to floor plan area is typically on the order of 1%. Fig. 3 displays the relation between the ratio of wall shear to total base shear V_w/V_t with wall index p and number of walls used in the system. It is seen in Fig. 3 that even if a few numbers of robust walls (L_w>3 m) are used in frame-wall buildings, the fraction of shear carried by wall is very high. When only three walls are used in the system, the shear force on the walls builds up to 60, 80 and 90% of the total base shear, if 3 m, 5 m and 8 m long walls are used in design, respectively. When 1% of wall index is provided, nearly all
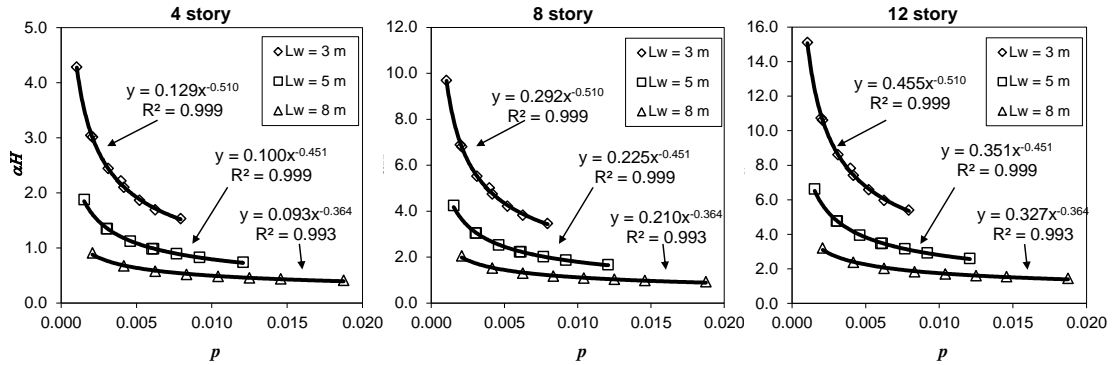
Fig. 2 Relation between the wall index (*p*) and behavior factor αH
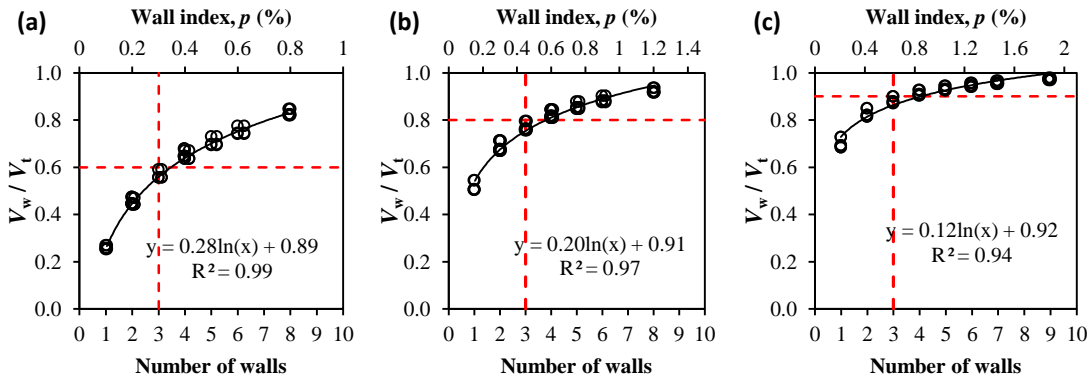
Fig. 3 Relation between the ratio of wall shear to total base shear V_w/V_t, wall index *p* and number of walls used in the system for a) L_w=3 m, b) L_w=5 m, c) L_w=8 m long walls

the shear force is carried by the walls. It is also seen that for the same wall index that is obtained by using wall with different lengths, the V_w/V_t ratio increases as the wall length increases. This is related to the increased moment of inertia of wider walls.

Frame-wall structures (dual systems) in Eurocode 8 (CEN 2004) are classified as wall-equivalent or frame-equivalent according to the wall to total base shear fraction. When wall shear is in the range $0.50V_t \leq V_w \leq 0.65V_t$, the system is named as wall-equivalent dual system, and when $V_w \geq 0.65V_t$ it is named as wall system in which both vertical and lateral loads are mainly resisted by vertical structural walls, either coupled or uncoupled. If the shear distribution is in the range $0.35V_t \leq V_w \leq 0.50V_t$, then structural system is classified as frame-equivalent dual system. According to this classification, although robust frame components are used, nearly all the models, except the one that is composed of single L_w=3 m long wall, are wall-equivalent dual system or mostly wall system. A frame-equivalent dual system can only obtained with shorter walls (L_w<3 m). This is the result of wall definition in Eurocode 8. A structural element supporting other elements and having an elongated cross-section with a length to thickness ratio L_w/t_w of greater than 4 is classified as a wall in Eurocode 8. According to this definition, a vertical structural element having 0.25×1.2 m dimensions is assumed to be a wall. Whereas this may be true in a 4-story building by no means such a member is a wall in a 12-story structure. So, a rational definition of wall should be based on

height to length ratio H_w/L_w (ASCE 41-06, 2006). In that sense this study covers frame-wall structures composed of wall members behaving as shear wall.

2.3 Design of single wall-equivalent frame models

Using the data produced on dynamic and static characteristic of frame-wall structures, variations in stiffness and yield strength along the height of the generic single wall-equivalent frame models were calculated. The primary variables in creating a model was the wall length (L_w), height (H_w), and wall index (p). Instead of wall height number of stories (N) can be used as well. It was considered that the generic equivalent frame-single wall models cover a wall index range of 0.002 to 0.02. Models that represent 4, 8 and 12 story structures were developed. The lengths of wall used in the design are 3 m, 5 m and 8 m. The frame-wall model is characterized by a particular wall index (p) and the parameter αH. The stages of model construction can be defined as follows:

1. Select a wall length (L_w) and wall index (p). In this study, a constant wall thickness t_w=0.25 m is adopted for all walls.

2. Decide the number of stories (N), i.e., height H of the model.

3. Compute the behavior factor (αH) using the selected wall index value and relations presented in Fig. 2.

4. The fundamental period of structure (T_1) is determined by Eq. (5) that is developed for frame-wall buildings (Kazaz and Yakut 2010)

$$T_1 = 0.00406 \frac{H}{L_w} N \frac{1}{\sqrt{p\left(1.875^2 + (\alpha H)^2\right)}}$$ (5)

1. For an assumed or given wall index (p) the floor area per wall is calculated as $A_f = L_w t_w / p$ for predetermined wall dimensions.

2. The story mass is calculated as $m_s = A_f . m_f$ (m_f=1 t/m^2). Story mass calculated in this way provides much better and realistic representation of lateral seismic loads acting on the wall, when compared to procedures that are based on tributary area concept or matching of a target period of typical structural system.

3. The typical values of axial load ratios in practice with cantilever walls are in the range $0 < P/A_w f_c \leq 0.15$ for low-to-medium height buildings. For simple calculation it can be assumed that each wall is subjected to 1~1.25 percent axial load ratio per story (Priestley *et al*. 2007). So the vertical load carried by the wall is calculated assuming that the axial load ratio at the base section of 4-, 8- and 12-story walls are 0.05, 0.10 and 0.15, respectively.

This completes the model generation. Next a simple yet straight-forward design procedure that incorporates moment and shear expression derived from the solution of Eq. (1) was used to quantify the seismic shear force distribution among the wall and frame components of the generic frame-wall models and to calculate the required amount of flexural reinforcement at the boundary elements of the walls. Design actions on the walls were determined using the equivalent static lateral load procedure described in Turkish Seismic Code (TSC 2007).

4. Total equivalent seismic load (base shear) acting on the entire frame-wall structure is obtained by

$$V_t = \frac{W \cdot A(T_1)}{R} \qquad (6)$$

where W is the total weight of the model calculated as $N.m_s.g$. $A(T_1)$ is the spectral acceleration coefficient that is obtained from the design spectrum given in Fig. 5. The design spectrum was generated assuming a local site class Z3 (firm soil) and Seismic Zone 1 (A_o=0.4, effective ground acceleration coefficient) according to TSC (2007). R is the seismic load reduction factor (structural behavior factor) given as 6 and 7 for buildings in which seismic loads are fully resisted by solid structural walls and seismic loads are resisted by combined frames and solid and/or coupled structural walls, respectively, for high ductility systems. For the sake of simplicity and consistency, a constant R equal to 6 was adopted. The total seismic base shear V_t is assumed to be distributed as an inverted triangle over the height of the model.

5. The bending moment and the shear force at the base of the wall is calculated with Eq. (2) and (4), respectively.

6. Considering the moment demands that arise during the dynamic response, a linear bending moment envelope is used in design. Additionally from the base of wall in a region that has a height equal to $H_{cr} = \max[L_w, H_w/6]$ but not greater than $2L_w$ a constant moment distribution is assumed considering the tension shift effect (TSC 2007).

7. It is assumed that the length of boundary elements is $0.2L_w$ at the edges and flexural reinforcement is distributed uniformly in the boundary element. The minimum boundary element longitudinal reinforcement ratio is set to ρ_b=0.005, which is lower than the code minimum 0.01, since unless this was done systems would be designed for much higher lateral strength than it was intended with R=6. It is aimed to increase the deformation vulnerability of models to seismic loads. The percentage of vertical and horizontal web reinforcement ratio (ρ_{sh}) is a constant value equal to 0.0025 unless extra shear reinforcement is required. Characteristic concrete compressive (f_c) and steel yield (f_y) material strengths are employed instead of design strengths. Concrete compressive and steel yield strength is taken as 25 MPa and 420 MPa, respectively.

8. The shear force on frame component V_f is obtained as the difference of V_t-V_w. The story yield strength is not constant along the height of the structure. It is distributed to the upper stories in proportion to design forces resulting from the code static lateral load pattern. The calculated frame shear force at the base story decreases considerably as the wall index (amount of wall) increases. However, it cannot be disregarded totally. From constructional point of view the minimum reinforcement detailing requirements govern.

An approximate rule was developed for a "typical situation". If it is considered that the minimum column dimension is 0.6×0.6 m^2 and minimum reinforcement amount is used $(\rho_b)_{min}$=0.01, the moment capacity of columns is found as 256, 305 and 345 kN-m for 5 percent, 10 percent and 15 percent axial load levels, respectively. If the contra-flexure height is assumed to occur at the mid height of the column, the column shears are found as 170, 203 and 230 kN for the same set of axial load levels, respectively. Considering that at least two columns accompany a wall in the system, the minimum story yield shear force due to columns for generic frame-wall structures are calculated as 340, 406 and 460 kN for 4-, 8- and 12-story structures, respectively. If the frame shear force found from elastic analysis is lower than the values given above, they are replaced with these ones. This excess strength is not foreseen by the elastic analysis used in the design. One of the consequences of this situation is that the actual force reduction factor (R) in the system may turn out to be smaller than that what is intended initially in the design of frame-wall systems.

The complete set of parameters that emerged from the design process and were used to define frame-wall models are given in Table A.1 in the APPENDIX.

2.4 Generic single wall-equivalent frame

While for linear analysis the analytical expressions derived for continuum shear-flexure beam model yields satisfactory results, for nonlinear case a discrete nonlinear type of simplified frame-wall model as presented in Fig. 4 was developed for the finite element analysis. The model was generated in SeismoStruct (SeismoSoft 2007). 3D displacement based beam-column elements capable of modeling members of space frames with geometric and material nonlinearities were used to model shear walls. The sectional stress-strain state of beam-column elements was obtained through the integration of the nonlinear uni-axial material response of the individual fibers into which the section has been subdivided, accounting for the spread of inelasticity along the member length and across the section depth. In the shear wall component, a story was divided into five elements allowing finer mesh in the regions of plastification as shown in Fig. 4. The frame component was modeled as combination of rigid frame elements interconnected with nonlinear shear links. The wall and frame components were connected with rigid links and a rotational spring was introduced to account for the link beam moments.

The story distortion angle–shear force (γ-F) relation for the link elements was idealized with the Takeda hysteresis model. Analysis results of typical frame–wall structure indicate that yielding of walls and the frames occur at different levels of lateral drift. The global yield displacement of the structures is largely determined by the yielding of beams. According to Priestley *et al.* (2007), the frame yield drift is given as, $\theta_{yFrame} = \gamma_y = 0.5 l_b \varepsilon_y / h_b$ where l_b is the average beam length and h_b is the average depth of the beams at the level of interest. When typical values were used (ε_y=0.0021, h_b=0.6 m, l_b=5 m), story yield drift is obtained as 0.0088. Aschheim (2002) states that the frames yields between 0.5 and 0.6 percent roof drift range regardless of the number of stories. For the story rotational angle (inter-story drift ratio) at yielding a value equal to 0.0067 is proposed
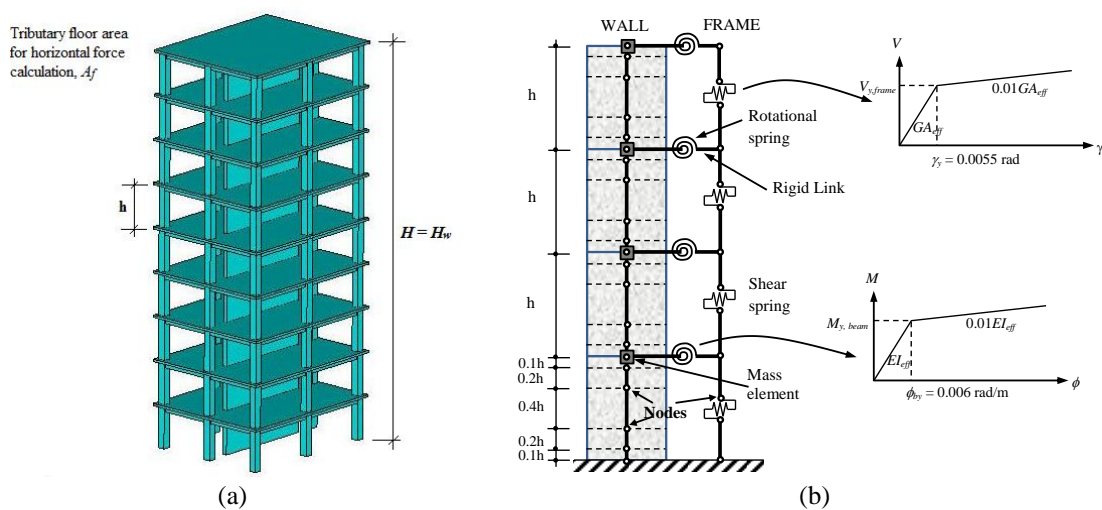
Fig. 4 (a) Frame per wall: single wall-equivalent frame, (b) Finite element model of the generic single wall-equivalent frame model.

by Akiyama (1987). In the light of this discussion, the yield story distortion angle (γ_y) was assumed to be 0.0055.

The yield curvature of link beams was calculated by the relation $\phi_{by}=1.7\varepsilon_y/h_b$ (Priestley *et al*. 2007). For the materials and section geometries adopted in this study ($\varepsilon_y=0.0021$ and $h_b=0.6$ m) the beam curvature at yield takes the value of 0.006 rad/m, which also agrees with the moment-curvature analyses of typical beam sections. The behavior of rotational springs used to model moments transferred from link beams were characterized by the Takeda hysteresis model. The yield strength of frames was distributed over the stories so that all would yield simultaneously under the static design earthquake forces.

3. Ground motion data set

In the selection of acceleration time-series to be used as input to dynamic analyses, spectral matching technique was used. It was assumed that the ground motion spectra matches the elastic response spectrum of TSC (2007) that is defined on firm soil site class Z3 ($T_A=0.15$ s and $T_B=T_C=0.6$ s) with *PGA* of 0.4 g for the design earthquake that has 10 percent probability of being exceeded in 50 years. The search was based on the average root-mean-square deviation of the observed spectrum from the target design spectrum. Even when the ground motions satisfactorily match the target spectral shape, their intensity may vary significantly. A scale factor (SF_{Spec}) defined as the average of the ratio of spectral ordinates of target and matching spectra at periods 0.1s, 0.4s and 0.85s was introduced. So, 215 ground motions compiled by Kazaz (2010) were screened for finding the spectrum compatible traces. 10 records conforming to the given limitations were selected and used as seismic input for response analyses. The acceleration response spectra of these scaled ground motions are presented in Fig. 5. In Table 1 peak ground values of unscaled strong motions records are given together with applied scale factors. Ground motions yielded an average *PGA/PGV* ratio of 8.2 s^{-1} with standard deviation of 1.0. After scaling, the ground motions have nearly uniformly distributed peak ground values, yielding mean values of 480.1 cm/s[2] and 58.9 cm/s for acceleration and velocity, respectively.

4. Nonlinear dynamic analysis of generic frame-wall models

The seismic demand characterized by the code spectrum compatible ground motions were applied on the set of single wall-equivalent frame models that represents broad range of frame-wall combinations of relative strength. The performance of wall elements was evaluated by comparing the response parameters with respect to code specified limits. These parameters include maximum roof drift ratio, base rotation and maximum compressive strain at the extreme fiber of the wall base section.

Fig. 6 displays the variation of maximum inter-story drift ratio *MIDR* of frame-wall models with respect to the wall index. The graphs reveal the decreasing tendency in the drift ratio with increasing wall area. The effect of increased wall amount in reducing drift demands is much more pronounced for 4-story models compared to 8- and 12-story models. This can be attributed to higher over-strength allocated in the design as a result of minimum reinforcement requirements. For 4-story models, the drift ratio demands reduce from approximately 1.75 to 0.5 percent with the increased wall area. For 8-story models the mean drift ratio reduces from 1.4 to 0.9 percent, 1.3 to

Table 1 Catalog data of the selected unscaled ground motions and applied scale factor

No	Earthquake	Year	M_w	Station	R_d (km)	PGA (cm/s^2)	PGV (cm/s)	SF_{Spec}
1	Imperial Valley	1979	6.5	Keystone Rd., El Centro Array #2	16.2	309	32.7	1.77
2	Kocaeli	1999	7.4	Duzce	17.1	308	50.7	1.52
3	Northridge	1994	6.7	Los Angeles, Brentwood V.A. Ho.	23.1	182	24.0	2.69
4	Northridge	1994	6.7	Pacoima-Kagel Canyon	10.6	424	50.9	1.20
5	Whittier Narrows	1987	6.1	7420 Jaboneria, Bell Gardens	16.4	216	28.0	1.98
6	Cape Mendocino	1992	7.1	89324 Rio Dell Overpass - FF	18.5	378	43.9	1.43
7	Northridge	1994	6.7	24389 LA - Century City CC North	25.7	218	25.2	2.11
8	Northridge	1994	6.7	24283 Moorpark - Fire Sta.	28	189	20.2	2.56
9	Loma Prieta	1989	6.9	Hollister Differential Array	25.8	274	35.6	1.47
10	Northridge	1994	6.7	LA - Fletcher Dr.	29.5	235	26.2	2.00
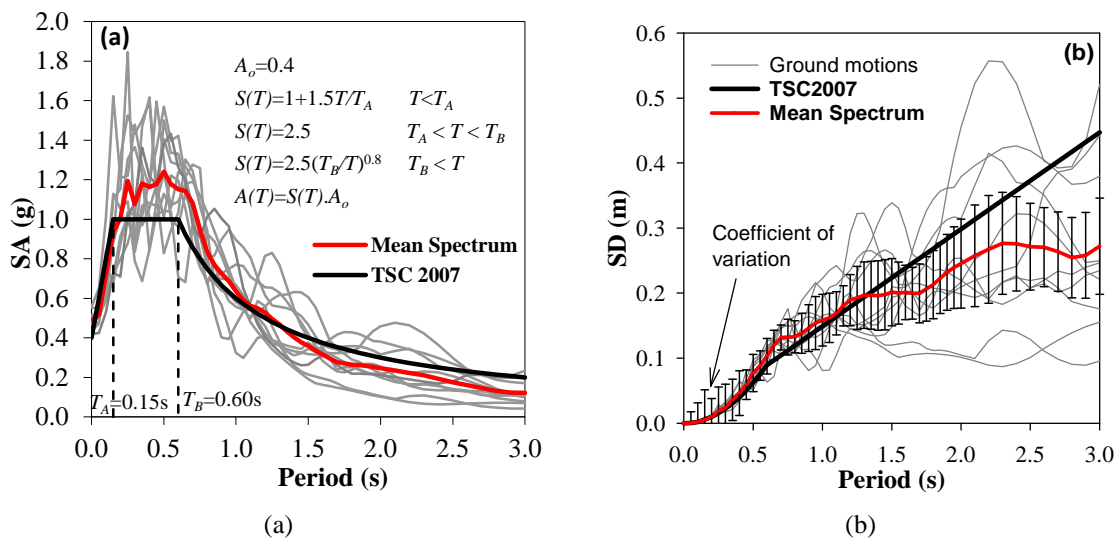
Fig. 5 (a) Acceleration, (b) Displacement response spectra of the scaled ground motions

0.8 percent, 1.2 to 0.8 percent for 3 m, 5 m and 8 m walls, respectively, as the wall index increases from 0.2 to 2 percent. The same relation between the wall index and inter-story drift ratio for 12-story models is observed as 1.4 to 0.81 percent, 1.3 to 0.75 percent, and 1.15 to 0.73 percent for 3 m, 5 m and 8 m walls, respectively. The average inter-story drift reduces to 1% or below for p>1.0%. Although the reduction is not so significant considering the increase in the wall area, the dispersion in the drift data becomes smaller indicating a better control over the drift ratio. For wall indexes greater than 0.8% the scatter of data around the mean drift ratio due to ground motion variability decreases significantly. This is mainly due to increase in the lateral stiffness of models that leads their fundamental period of vibration to fall in a zone of the response spectra that has smaller dispersion as shown in Fig. 5(b).

There is a slight reducing effect of wall length (rigidity) on drift demands of 8 and 12-story

models, which is much more pronounced in 4-story walls. On the other hand, larger wall length is very effective in reducing drift in linear analysis (Kazaz 2010). In general, the mean seismic *MIDR* decrease from 1.5 to 0.75 percent as the wall index increases from 0.2 to 2 percent. For wall indexes larger than 1.0 percent the *MIDR* is in the order of 1% or less. It should be reminded that the minimum boundary element longitudinal reinforcement ratio is taken as 0.005, which is specified as 0.01 in the code. So if code value is adopted in the models, it is expected that the drift demands will be lower in the models with *p*>1%.

Fig. 7 displays the plastic rotation demand at the base of walls plotted against the wall index. The ASCE 41-06 (2006) plastic rotation limits for immediate occupancy (IO), life safety (LS), collapse prevention (CP) performance levels were also superimposed on the same figure to facilitate estimation of likely performance of walls in different structural systems. The ASCE 41-06 limits for each model structure were calculated using normalized shear stress (v) and the axial load ratio (P/P_o) on the wall element. The normalized shear stress is calculated according to $v = V_{\max}/t_w L_w \sqrt{f_c}$ using maximum dynamic wall shear force obtained from analyses. As seen in Fig. 7 the calculated ASCE 41-06 plastic rotation limits indicate very low deformability at the base of the walls for low wall index systems ($p<0.5\%$) especially for 8- and 12-story structures. This is due to high shear stress carried by the walls in this range. Above $p=0.5\%$ nearly all walls in all systems assure at least life safety (LS) performance level for mean plastic rotation demand.
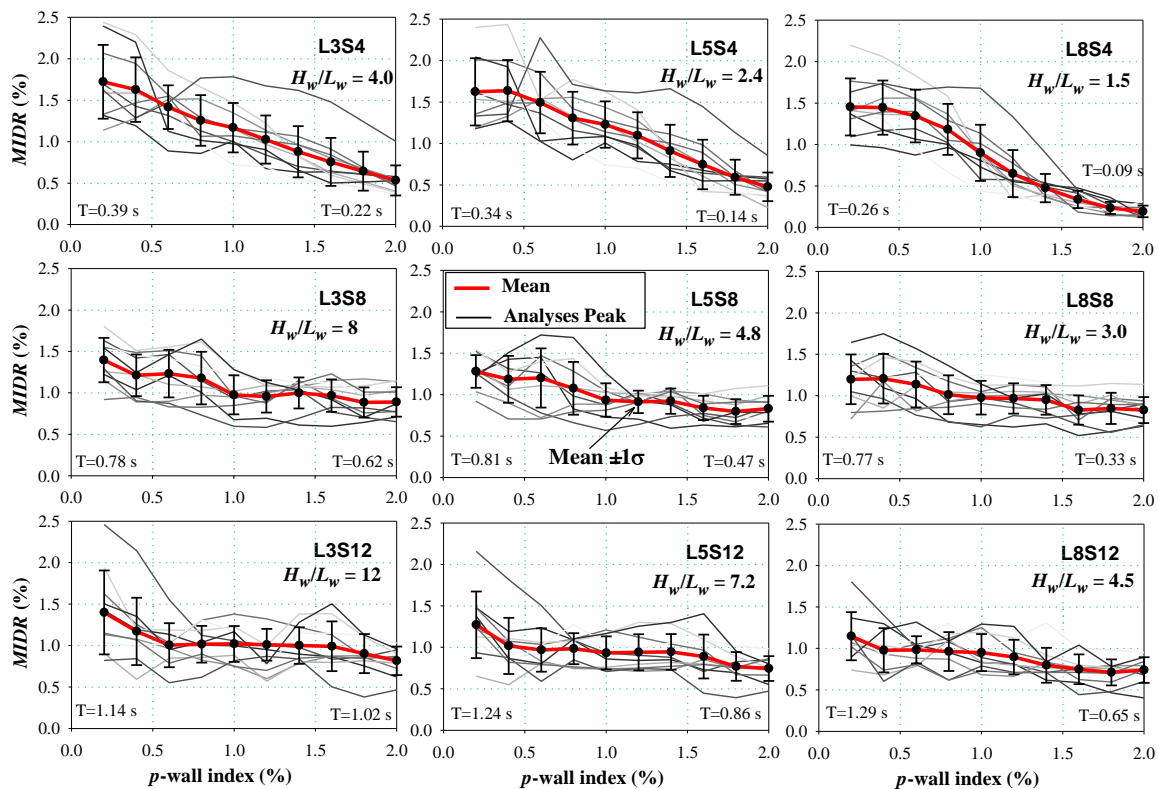
Fig. 6 Variation of maximum inter-story drift ratio with wall index and number of stories. In "L3S4", L3 indicates 3 m wall length and S4 refers to 4-story structure. The other labels should be read accordingly

When the deviation from the mean response is considered wall index greater than 1.0% is required for LS performance level.

The plastic rotation capacity of the structural walls with conforming boundary elements were calculated according to the expression given in Eq. (7) (Kazaz *et al.* 2012) and plotted on Fig. 7 as well. In the derivation of Eq. (7) nonlinear material behavior like crushing and cracking of concrete, buckling and rupture of reinforcing bars were taken into account

$$\theta_p = A\left(\rho_b\right)^B . e^{-(C\nu + DL_w)} \mp \sigma\left(\theta_p\right) \tag{7}$$

In this equation *A*, *B*, *C* and *D* are coefficients defined in Table 2 as a function of axial load ratio (P/P_o). ρ_b is the boundary element reinforcement ratio, ν is the normalized shear stress and L_w is the wall length. The following set of equations can be employed in the calculation of standard deviation of plastic rotation $\sigma(\theta_p)$

$$\sigma(\theta_p) = \begin{cases} 0.1429\theta_p + 0.0005 & if\ \theta_p \le 0.014 rad \\ 0.0025 & if\ 0.014 rad < \theta_p \le 0.03 rad \\ 0.8125\theta_p - 0.0219 & if\ 0.03 rad < \theta_p \le 0.038 rad \\ 0 & if\ 0.038 rad < \theta_p \end{cases} \tag{8}$$
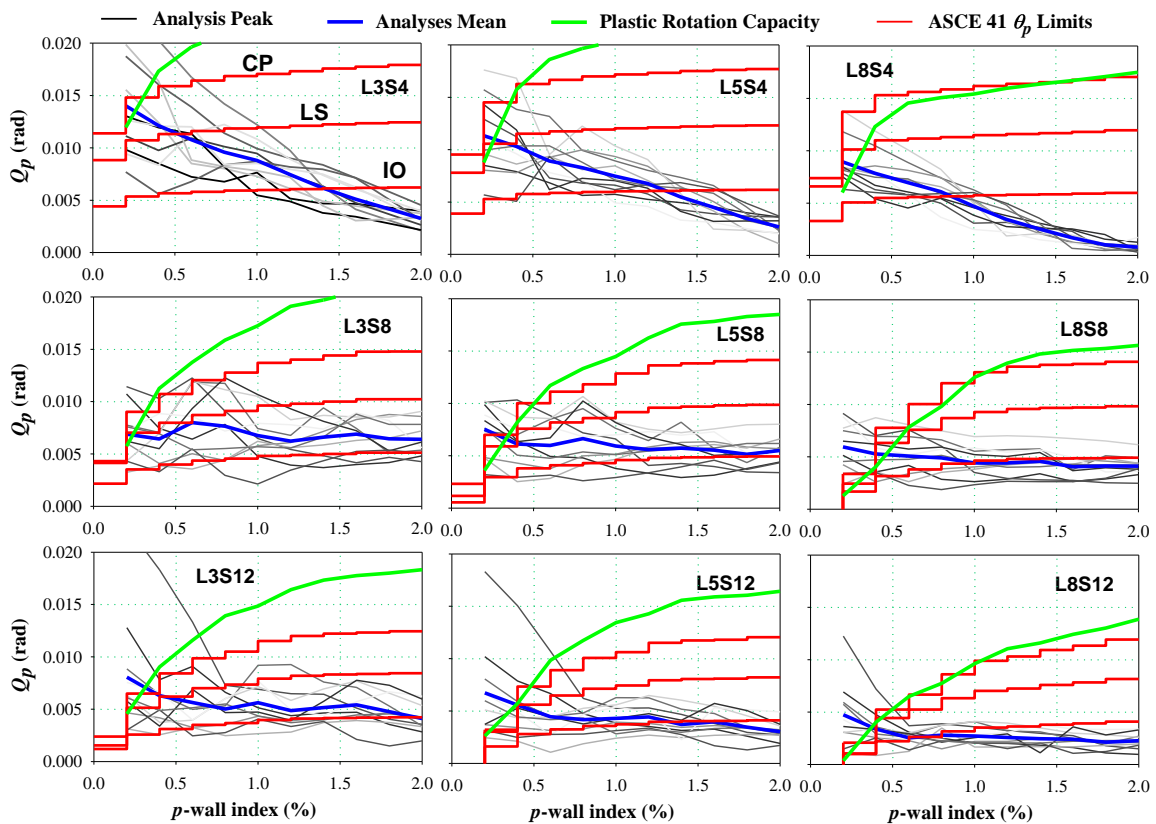
Fig. 7 Comparison of mean base rotation demand at the wall base with ASCE/SEI 41 performance limits

Table 2 Coefficients of Eq. (7)

P/P_o	A	B	C	D
≤0.10	0.138	0.220	1.814	0.071
=0.15	0.087	0.148	1.779	0.066
=0.25	0.034	0.037	1.485	0.037

The maximum compressive strains at the extreme fiber of wall base section are plotted in Fig. 8. The pronounced effect of high shear stress is quite obvious on the increased strain demand in low wall index structures. The frame-wall interaction results in an increase in the slope of the moment profile along the lower stories of the wall, and thus increases the level of shear stress that must be resisted by the wall when compared to cantilever wall. The base stories of walls in frame-wall structures with $p<0.6\%$ resemble squat wall in terms of loading conditions, so they inhabit very low deformation capacity (drift ratio<0.0075). Analysis results indicate that most of the damage concentrates in the compression zone leading to concrete crushing, loss of concrete integrity at this region. This indicates that longitudinal bars are more susceptible to buckling in such cases. Although frame-wall structures display a superior performance over the ductile frame under low to moderate seismic actions (Lu 2002), the low wall indexed frame-wall structure deteriorates more rapidly than the bare frame during advanced inelastic response. The rocking of
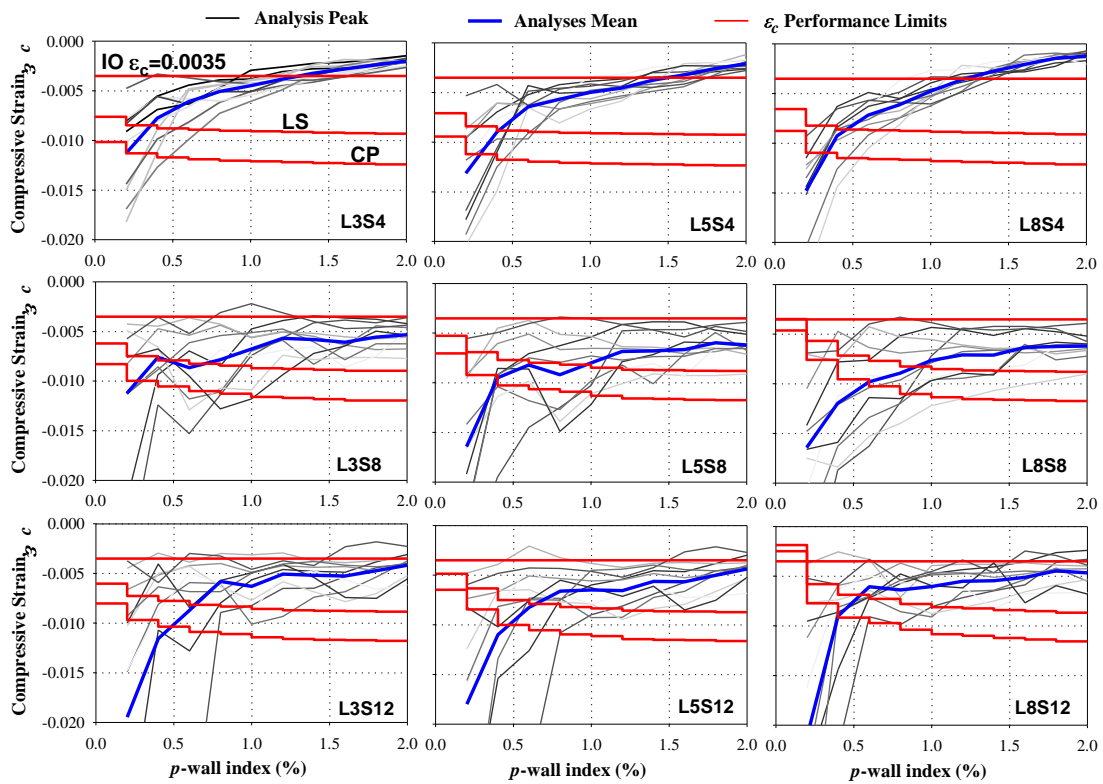
Fig. 8 Comparison of maximum compressive strains and strain limits at the base section

the wall occurs as a result of concentrated plastic hinge deformations. The rocking of the wall results in severe material damage at localized critical regions. As seen in Fig. 8, concrete compressive strains in low wall index frame-wall structures are much higher than the limit allowed for design (ε_c=0.003), so it can be concluded that while using walls together with frames a minimum requirement must be sought on the amount of walls with respect to the total floor area. The limiting value can be recommended as p=0.6%.

Compression strain damage limits plotted on Fig. 8 is calculated according to Kazaz and Gülkan (2012b). Priestley *et al.* (2007), assuming that the useful limit for confined concrete in compression is determined by the fracture of the transverse reinforcement confining the core, derived the following expression by equating the strain energies of the concrete and confining steel absorbed in a unit volume of core concrete

$$\varepsilon_{cu} = 0.004 + 1.4 \frac{\rho_s f_{yw} \varepsilon_{su}}{f_{cc}} \tag{9}$$

where f_{yw} is the yield strength of transverse steel, ρ_s is the volumetric ratio of boundary element transverse reinforcement, ε_{su} is the strain at maximum stress of the reinforcing steel and f_{cc} is the compressive strength of confined concrete. Based on this expression, Turkish Seismic Code specifies strain limits to evaluate the performance of reinforced concrete members. In TSC the concrete strain limits at the fibers of a cross section for collapse limit CP is given by

$$\left(\varepsilon_c\right)_{CP} = 0.004 + 0.014\left(\rho_s / \rho_{sm}\right) \leq 0.018 \tag{10}$$

where ε_c is the concrete strain at the outer fiber of the confined core and ρ_s/ρ_{sm} is the ratio of existing confinement reinforcement at the section boundary to the confinement required by the TSC 2007. Kazaz and Gülkan (2012b) displayed that neither Eq. (9) nor Eq. (10) provides conservative estimates of the concrete compression strains at the extreme fiber for shear walls, and proposed the following expression as a lower bound prediction of the compressive strain as a function of shear stress and amount of confinement reinforcement using the results of extensive finite element analyses on shear wall models and experimental data (Kazaz *et al.* 2012, Kazaz and Gülkan 2012b). The compression strain limits at life safety (LS) and collapse prevention (CP) performance levels for conforming members is given as

$$\left(\varepsilon_c\right)_{LS} = 0.010 - 0.005\nu \tag{11}$$

$$\left(\varepsilon_c\right)_{CP\max} = 0.0135 - 0.006\nu \tag{12}$$

here ν is the normalized shear stress. If the volumetric ratio of the confinement reinforcement is lower than $\rho_s \leq 0.01$ than a conservative lower bound value of the ultimate compression strain can be estimated using

$$\left(\varepsilon_c\right)_{CP} = 0.004 + 100\rho_s\left[0.0095 - 0.006\nu\right] \qquad if \qquad \rho_s < 0.01 \tag{13}$$

In such nonconforming cases, the concrete compression strain limit at life safety performance level can be taken as 70% of the ultimate compression strain, $(\varepsilon_c)_{CP}$.

5. Discussion of results

Seismic demand in this study is characterized by the design earthquake that has 10 percent probability of being exceeded in 50 years as shown in Fig. 5. This corresponds to a major earthquake, under which the main members may sustain severe damage, but the building should not collapse and life safety is guaranteed by controlling the damage. TSC (2007) establishes the performance criteria as Life Safety (LS) for this level of earthquake intensity. It is recently reported that many modern RC shear wall buildings suffered severe damage, mainly in the form of concrete cover spalling, followed by longitudinal boundary bar buckling and concrete crushing during the 27 February 2010 Chilean moment magnitude 8.8 earthquake (Massone 2013). In the following, based on the concrete compression strains at the extreme fiber of the section,

Table 3 Statistical evaluation of maximum concrete compression strain values from analyses

	p	ε_μ	ε_σ	$(\varepsilon_c)_{LS}$	$\frac{(\varepsilon_\mu-\varepsilon_\sigma)}{(\varepsilon_c)_{LS}}$	ε_μ	ε_σ	$(\varepsilon_c)_{LS}$	$\frac{(\varepsilon_\mu-\varepsilon_\sigma)}{(\varepsilon_c)_{LS}}$	ε_μ	ε_σ	$(\varepsilon_c)_{LS}$	$\frac{(\varepsilon_\mu-\varepsilon_\sigma)}{(\varepsilon_c)_{LS}}$
			L_w=3 m					L_w=5 m				L_w=8 m	
4-story	0.002	-0.0113	0.0045	-0.0072	2.19	-0.0131	0.0051	-0.0066	2.76	-0.0148	0.0043	-0.0060	3.15
	0.004	-0.0078	0.0029	-0.0082	1.31	-0.0090	0.0033	-0.0081	1.52	-0.0093	0.0025	-0.0079	1.49
	0.006	**-0.0061**	**0.0019**	**-0.0085**	**0.94**	**-0.0064**	**0.0017**	**-0.0086**	**0.95**	**-0.0072**	**0.0017**	**-0.0083**	**1.07**
	0.008	-0.0051	0.0011	-0.0087	0.71	-0.0057	0.0012	-0.0087	0.79	-0.0061	0.0013	-0.0084	0.89
	0.01	-0.0045	0.0009	-0.0088	0.61	-0.0050	0.0011	-0.0088	0.69	-0.0047	0.0011	-0.0085	0.69
	0.012	-0.0038	0.0007	-0.0088	0.52	-0.0045	0.0009	-0.0089	0.61	-0.0036	0.0009	-0.0086	0.52
	0.014	-0.0032	0.0007	-0.0089	0.44	-0.0038	0.0008	-0.0089	0.51	-0.0028	0.0005	-0.0087	0.38
	0.016	-0.0028	0.0006	-0.0090	0.38	-0.0032	0.0008	-0.0089	0.45	-0.0021	0.0005	-0.0087	0.30
	0.018	-0.0024	0.0005	-0.0090	0.32	-0.0026	0.0005	-0.0090	0.34	-0.0015	0.0004	-0.0088	0.21
	0.02	-0.0020	0.0004	-0.0091	0.26	-0.0021	0.0005	-0.0090	0.29	-0.0012	0.0004	-0.0089	0.19
8-story	0.002	-0.0112	0.0080	-0.0057	3.40	-0.0164	0.0071	-0.0046	5.10	-0.0164	0.0077	-0.0026	9.31
	0.004	-0.0076	0.0029	-0.0071	1.48	-0.0095	0.0043	-0.0064	2.14	-0.0120	0.0051	-0.0051	3.37
	0.006	-0.0087	0.0038	-0.0075	1.65	-0.0082	0.0035	-0.0073	1.60	-0.0098	0.0044	-0.0067	2.11
	0.008	-0.0078	0.0035	-0.0079	1.43	-0.0092	0.0040	-0.0076	1.73	-0.0089	0.0036	-0.0073	1.72
	0.01	-0.0068	0.0029	-0.0081	1.18	-0.0080	0.0028	-0.0078	1.38	-0.0076	0.0027	-0.0079	1.30
	0.012	**-0.0057**	**0.0018**	**-0.0084**	**0.89**	-0.0068	0.0020	-0.0082	1.09	-0.0071	0.0024	-0.0082	1.16
	0.014	-0.0058	0.0017	-0.0085	0.88	-0.0068	0.0020	-0.0084	1.05	-0.0071	0.0022	-0.0084	1.11
	0.016	-0.0061	0.0017	-0.0086	0.90	**-0.0067**	**0.0018**	**-0.0084**	**1.00**	**-0.0063**	**0.0018**	**-0.0084**	**0.97**
	0.018	-0.0056	0.0014	-0.0087	0.80	-0.0060	0.0015	-0.0085	0.88	-0.0062	0.0016	-0.0085	0.93
	0.02	-0.0053	0.0013	-0.0087	0.76	-0.0062	0.0014	-0.0085	0.89	-0.0062	0.0013	-0.0085	0.88
12-story	0.002	-0.0195	0.0256	-0.0054	8.29	-0.0180	0.0135	-0.0042	7.60	-0.0211	0.0208	-0.0028	14.84
	0.004	-0.0116	0.0167	-0.0068	4.14	-0.0110	0.0084	-0.0058	3.35	-0.0090	0.0056	-0.0052	2.81
	0.006	-0.0087	0.0089	-0.0074	2.39	-0.0082	0.0066	-0.0071	2.09	-0.0061	0.0018	-0.0064	1.24
	0.008	-0.0058	0.0019	-0.0078	0.99	-0.0066	0.0021	-0.0075	1.16	-0.0064	0.0019	-0.0068	1.21
	0.01	**-0.0063**	**0.0022**	**-0.0080**	**1.07**	-0.0065	0.0019	-0.0079	1.07	**-0.0060**	**0.0019**	**-0.0074**	**1.07**
	0.012	-0.0051	0.0018	-0.0083	0.83	**-0.0066**	**0.0019**	**-0.0080**	**1.06**	-0.0055	0.0016	-0.0078	0.91
	0.014	-0.0052	0.0013	-0.0084	0.77	-0.0056	0.0016	-0.0083	0.87	-0.0055	0.0016	-0.0079	0.89
	0.016	-0.0053	0.0017	-0.0085	0.82	-0.0057	0.0019	-0.0083	0.91	-0.0051	0.0016	-0.0081	0.83
	0.018	-0.0047	0.0014	-0.0085	0.72	-0.0050	0.0017	-0.0084	0.80	-0.0045	0.0013	-0.0082	0.71
	0.02	-0.0042	0.0012	-0.0086	0.62	-0.0044	0.0012	-0.0084	0.66	-0.0047	0.0014	-0.0084	0.72

performances of the models were evaluated.

Table 3 displays the mean compression strain (ε_μ), it's standard deviation (ε_σ) and the life safety performance criteria (ε_c)$_{LS}$ calculated for each model that was characterized by a particular wall index (p). A performance index defined as (ε_μ-ε_σ)/(ε_c)$_{LS}$ was also introduced. If this value is greater than one, it is decided that the model does not conform life safety criteria. When 4-story frame-wall structures are provided with minimum of 0.6% wall index, LS performance level is ensured. For 12-story structures, wall index greater than 1% is necessary to satisfy the same criteria. In the medium heights, for 8-story frame wall structures higher amounts of walls area is required to control the damage, which is greater than 1.2% for L_w=3 m and 1.6% for L_w=5 m and L_w=8 m long walls. The periods of 8-story models are in the range of 0.3 to 0.8 s. These periods fall into the acceleration controlled region of the spectrum, where the seismic forces become the highest. Another observation with regards to Table 3 is that for structural wall members with conforming boundary elements under the effect of moderate axial load levels, LS performance level can be conservatively defined (lower bound estimate) on the moment-curvature curve where the concrete compression strain reaches to ε_μ+ε_σ≈0.009, approximately.

Another conclusion derived from Table 3 is in regards to base shear distribution between the wall and frame components. It was displayed that for medium height structures, when frames and walls used together, the ratio of wall area to the total floor area greater than 0.6% is required to prevent excessive damage to the walls. It is also presented in Table A.1 that for such type of structures the ratio of wall shear to the total base shear V_w/V_b has a minimum value of 0.75 for different arrangements. When cracking and inelastic behavior of the members are considered this value can be reduced to 0.6 (Emori and Schnobrich 1981). Variation of the fraction of base shear carried by walls is displayed in Fig. 3. As an example, when only two L_w=3 m walls used in the plan configuration with area A_f=15×48=720 m^2, the resulting wall index and V_w/V_b is 0.0021 and 0.5, respectively. Lower base shear ratios can be only achieved by using smaller length walls (L_w<1.5 m) in the system. However these walls will experience significant shear and flexural deformations as a result of increased moment gradient at the lower stories. Concrete crushing and buckling of longitudinal bars is inevitable for low wall index systems. So in high seismicity regions, structures that have an elastic wall shear to the total base shear ratio V_w/V_b smaller than 0.6 will be avoided.

6. Conclusions

Seismic deformation demands on frame-wall buildings were investigated. Dynamic analysis results have demonstrated that when frame-wall systems resist lateral earthquake effects together, critical deformation demands may arise at the base of the walls for systems with low wall index that is defined as the ratio of total wall area to the floor area in plan in the direction of excitation. In addition to the interaction between the frames and walls at story levels, the shear and moment transferred from link beams extending from frames directly to the edges of the walls can significantly change the moment profile causing a reduction in the inflection height of the wall and increase in the slope of the moment curve. The resulting high shear stress conditions at the lower stories lead to limited deformability of wall members.

Considering the deformations, shear walls are very effective in reducing the seismically induced lateral drift in low-rise frame-wall systems. For medium rise buildings use of shear walls leads to well-controlled lateral drift and is very effective in reducing the dispersion in the drift due

to ground motion uncertainty as the wall index increases. The calculated average roof drift decreased from 1.5% to 0.5% for 4-story model. The average drift ratio in 8- and 12-story models has changed from approximately 1.4% to 0.75%. The study concludes that roof drift ratios less than 1% are likely during a major earthquake event for midrise buildings with ratios of wall area to floor plan area in one direction exceeding 1.0%. For structures whose period coincides with the constant acceleration region the wall area ratio will be greater than 1.5% to achieve life safety performance criteria as required by the code.

In frame-wall systems where walls are connected to the frames by link beams extending from ends, the minimum wall area in one direction will not be lower than 0.6% of the floor plan area to prevent the concrete crushing at the boundaries. Concrete compressive strains calculated in all frame-wall structures were much higher than the limit allowed for design, ε_c=0.003, which indicates to the need of confined boundary elements in walls. For structural wall members with conforming boundary elements, LS performance level can be conservatively defined on the moment-curvature curve with the point where the concrete compression strain reaches to 0.009, approximately, under the effect of moderate axial load levels.

Acknowledgements

References

Aschheim, M.A. (2002), "Seismic design based on the yield displacement", *Earthq. Spectra*, **18**(4), 581-600.

Akiyama, H. (1987), *Earthquake-Resistant Limit-State Design for Buildings*, Tokyo: University of Tokyo Press.

ASCE 41-06 (2006), *Seismic rehabilitation of existing buildings*, American Society of Civil Engineers, Reston, Virginia.

CEN/EN1998-1 (2004), *Eurocode 8: Design of structures for earthquake resistance - Part1: General rules, seismic actions and rules for buildings*, European Committee for Standardization, Brussels, Belgium.

Charney, F.A. and Bertero V.V. (1982) *An evaluation of the design and analytical seismic response of a seven-story reinforced concrete frame-wall structure*, UCB/EERC-82/08, Earthquake Engineering Research Center, University of California, Berkeley.

Dashti, F., Dhakal R.P. and Pampanin S. (2014), "Comparative in-plane pushover response of a typical RC rectangular wall designed by different standards", *Earthq. Struct.*, **7**(5), 667-689.

Emori, K. and Schnobrich, W.C. (1981), "Inelastic behavior of concrete frame-wall structures", *J. Struct. Eng.*, ASCE, **107**(1), 145-164.

Heidebrecht, A.C. and Stafford Smith, B. (1973), "Approximate analyses of tall wall-frame structures", *J. Struct. Eng.*, ASCE, **99**(2), 199-221.

Inel, M., Bilgin, H. and Ozmen, H.B. (2008), "Seismic capacity evaluation of school buildings in Turkey", *Proc. ICE-Struct. Build.*, **161**(3), 147-159.

Kayal, S. (1986), "Nonlinear interaction of RC frame-wall structure", *J. Struct. Eng.*, ASCE, **112**(5), 1021-1035.

Kazaz, İ. (2010), "Dynamic characteristics and performance assessment of reinforced concrete structural walls", Ph.D. thesis, Civil Engineering Department, Middle East Technical University, Ankara, Turkey.

Kazaz, İ., Gülkan, P. and Yakut, A. (2012), "Performance limits for structural walls: An analytical

perspective", *Eng. Struct.*, **43**, 105-119.

Kazaz, İ. and Gülkan, P. (2012a), "An improved frame-shear wall model: continuum approach", *Struct. Des. Tall Spec. Build.*, **21**(7), 524-542.

Kazaz, İ. and Gülkan, P. (2012b), "Damage limits for ductile reinforced concrete shear walls", *İMO Teknik Dergi*, **23**(4), 6113-6140. (in Turkish)

Kazaz, İ. and Yakut, A. (2010), "Evaluation of period formula for shear wall buildings", *9th US National and 10th Canadian Conference on Earthquake Engineering*, Toronto, Canada.

Khan, F.R., and Sbarounis, J.A. (1964), "Interaction of shear walls and frames", *Proc. ASCE*, **90**(3), 285-335.

Lalaj, O., Yardım, Y. and Yilmaz, S. (2015), "Recent perspectives for ferrocement", *Res. Eng Struct. Mat.*, **1**(1), 11-23.

Lazzali, F. (2013), "Seismic vulnerability of Algerian reinforced concrete houses", *Earthq. Struct.*, **5**(5), 571-588.

Lu, Y. (2002), "Seismic behavior of multistorey RC wall-frame system versus bare ductile frame system", *Earthq. Eng. Struct. Dyn.*, **31**(1), 79-97.

Massone, L.M. (2013), "Fundamental principles of the reinforced concrete design code changes in Chile following the Mw 8.8 earthquake in 2010", *Eng. Struct.*, **56**, 1335-1345.

Miranda, E. and Reyes, C.J. (2002), "Approximate lateral drift demands in multi-story buildings with nonuniform stiffness", *J. Struct. Eng.*, **128**(7), 840-849.

Özdemir, G. and Bayhan, B. (2015), "Response of an isolated structure with deteriorating hysteretic isolator model", *Res. Eng. Struct. Mat.*, **1**(1), 1-9.

Ozmen, H.B., Inel, M. and Cayci, B.T. (2013), "Engineering implications of the RC building damages after 2011 Van Earthquakes", *Earthq. Struct.*, **5**(3), 297-319.

Priestley, M.J.N., Calvi, G.M. and Kowalsky, M.J. (2007), *Displacement-based seismic design of structures*, Pavia, Italy, IUSS Press.

SeismoSoft (2007), *SeismoStruct: A computer program for static and dynamic nonlinear analysis of framed structures*, (online): Available from URL: www.seismosoft.com

Sozen, M.A. (1989), "Earthquake response of buildings with robust walls", *Fifth Chilean Conference on Earthquake Engineering*, Santiago, Chile.

Takabatake, H. (2010), "Two-dimensional rod theory for approximate analysis of building structures", *Earthq. Struct.*, **1**(1), 1-19.

TSC (2007), *Turkish Seismic Design Code for Buildings*, Ministry of Public Works and Resettlement, Ankara, Turkey.

Vallenas, M.V., Bertero, V.V. and Popov, E.P. (1979), "Hysteretic behavior of reinforced concrete structural walls", UCB/EERC Report 79/20, Earthquake Engineering Research Center, University of California, Berkeley.

Wallace J.W. and Moehle, J.P. (1992), "Ductility and detailing requirements of bearing wall buildings", *J. Struct. Eng.*, ASCE, **118**(6), 1625-1644.

CC

Appendix

Table A1 Strength and stiffness characteristics of frame-wall models developed for dynamic analysis, 4-story models

L_w (m)	H_w (m)	N_s	H_w/L_w	p (%)	αH	T_e (s)	A_f (m²)	V_b (kN)	R	V_b/R (kN)	M_w (kN-m)	V_w (kN)	V_f (kN)	V_w/V_b	P/P_o	P_o (kN)	ρ_b	ρ_{sh}	M_{beam} (kN-m)	K_{frame} (kN/m)	K_{beam} kN-m/rad	R_{exist}
3	12	4	4	0.2	2.85	0.39	375	14715	6	2453	6138	1341	1111	0.55	0.05	938	0.0263	0.0031	902	49381	225381	5.83
3	12	4	4	0.4	2.02	0.35	188	7358	6	1226	4431	886	340	0.72	0.05	938	0.0154	0.0025	706	15128	176554	5.87
3	12	4	4	0.6	1.65	0.32	125	4905	6	818	3515	654	164	0.80	0.05	938	0.0096	0.0025	598	7279	149525	4.40
3	12	4	4	0.8	1.43	0.29	94	3679	6	613	2938	517	96	0.84	0.05	938	0.0059	0.0025	523	4267	130830	3.58
3	12	4	4	1.0	1.28	0.28	75	2943	6	491	2535	428	63	0.87	0.05	938	0.005	0.0025	467	2796	116728	2.94
3	12	4	4	1.2	1.17	0.26	63	2453	6	409	2236	364	44	0.89	0.05	938	0.005	0.0025	422	1969	105570	2.50
3	12	4	4	1.4	1.08	0.25	54	2102	6	350	2004	318	33	0.91	0.05	938	0.005	0.0025	386	1458	96462	2.18
3	12	4	4	1.6	1.01	0.23	47	1839	6	307	1817	281	25	0.92	0.05	938	0.005	0.0025	355	1121	88859	1.93
3	12	4	4	1.8	0.95	0.22	42	1635	6	273	1663	253	20	0.93	0.05	938	0.005	0.0025	330	887	82401	1.72
3	12	4	4	2.0	0.90	0.22	38	1472	6	245	1535	229	16	0.93	0.05	938	0.005	0.0025	307	718	76840	1.55
5	12	4	2.4	0.2	1.53	0.34	625	24525	6	4088	17061	2739	1349	0.67	0.05	1563	0.0243	0.0045	992	59934	247949	6.12
5	12	4	2.4	0.4	1.13	0.27	313	12263	6	2044	11000	1680	364	0.82	0.05	1563	0.0114	0.0025	671	16187	167646	6.29
5	12	4	2.4	0.6	0.94	0.23	208	8175	6	1363	8185	1200	163	0.88	0.05	1563	0.0054	0.0025	514	7236	128507	5.26
5	12	4	2.4	0.8	0.83	0.21	156	6131	6	1022	6542	931	91	0.91	0.05	1563	0.005	0.0025	419	4028	104680	4.06
5	12	4	2.4	1.0	0.75	0.19	125	4905	6	818	5457	760	57	0.93	0.05	1563	0.005	0.0025	354	2539	88498	3.45
5	12	4	2.4	1.2	0.70	0.18	104	4088	6	681	4686	642	39	0.94	0.05	1563	0.005	0.0025	307	1734	76741	2.92
5	12	4	2.4	1.4	0.65	0.16	89	3504	6	584	4109	556	28	0.95	0.05	1563	0.005	0.0025	307	1253	76741	2.51
5	12	4	2.4	1.6	0.61	0.15	78	3066	6	511	3659	490	21	0.96	0.05	1563	0.005	0.0025	307	944	76741	2.19
5	12	4	2.4	1.8	0.58	0.15	69	2685	5.9	456	3312	439	17	0.96	0.05	1563	0.005	0.0025	307	737	76741	1.92
5	12	4	2.4	2.0	0.56	0.14	63	2349	5.7	413	3038	400	13	0.97	0.05	1563	0.005	0.0025	307	592	76741	1.68
8	12	4	1.5	0.2	0.84	0.26	1000	39240	6	6540	39936	5300	1240	0.81	0.05	2500	0.0259	0.0060	1002	55126	250614	5.60
8	12	4	1.5	0.4	0.66	0.19	500	19620	6	3270	22573	2976	294	0.91	0.05	2500	0.0096	0.0025	573	13077	143295	5.17
8	12	4	1.5	0.6	0.57	0.16	333	13080	6	2180	15799	2056	124	0.94	0.05	2500	0.005	0.0025	405	5495	101174	4.55
8	12	4	1.5	0.8	0.51	0.14	250	9375	5.7	1654	12317	1587	67	0.96	0.05	2500	0.005	0.0025	317	2982	79349	3.49
8	12	4	1.5	1.0	0.47	0.13	200	7064	5.3	1345	10193	1303	42	0.97	0.05	2500	0.005	0.0025	264	1863	65960	2.63
8	12	4	1.5	1.2	0.44	0.11	167	5615	4.9	1137	8721	1108	29	0.97	0.05	2500	0.005	0.0025	226	1267	56619	2.09
8	12	4	1.5	1.4	0.42	0.11	143	4631	4.7	986	7636	966	21	0.98	0.05	2500	0.005	0.0025	199	914	49707	1.72
8	12	4	1.5	1.6	0.40	0.10	125	3922	4.5	872	6802	857	15	0.98	0.05	2500	0.005	0.0025	177	688	44374	1.46
8	12	4	1.5	1.8	0.38	0.09	111	3390	4.3	783	6140	771	12	0.98	0.05	2500	0.005	0.0025	161	536	40125	1.26
8	12	4	1.5	2.0	0.37	0.09	100	2978	4.2	710	5601	701	10	0.99	0.05	2500	0.005	0.0025	147	428	36656	1.11

Table A1 Continued

L_w (m)	H_w (m)	N_s	H_w/L_w	p (%)	αH	T_e (s)	A_f (m²)	V_b (kN)	R	V_b/R (kN)	M_w (kN-m)	V_w (kN)	V_f (kN)	V_w/V_b	P/P_o	P_o (kN)	ρ_b	ρ_{sh}	M_{beam} (kN-m)	K_{frame} (kN/m)	K_{beam} kN-m/rad	R_{exist}
3	24	8	8	0.2	6.44	0.78	375	23905	6	3984	10831	1990	1995	0.50	0.1	1875	0.0495	0.0061	1895	88653	473812	5.69
3	24	8	8	0.4	4.56	0.75	188	12261	6	2044	8385	1388	655	0.68	0.1	1875	0.0339	0.0033	1587	29113	396773	5.57
3	24	8	8	0.6	3.73	0.73	125	8369	6	1395	7000	1063	332	0.76	0.1	1875	0.0250	0.0025	1405	14738	351174	4.70
3	24	8	8	0.8	3.23	0.71	94	6417	6	1069	6111	866	203	0.81	0.1	1875	0.0194	0.0025	1279	9023	319848	4.09
3	24	8	8	1.0	2.89	0.69	75	5242	6	874	5487	735	138	0.84	0.1	1875	0.0154	0.0025	1186	6153	296614	3.50
3	24	8	8	1.2	2.64	0.68	63	4455	6	743	5021	641	101	0.86	0.1	1875	0.0124	0.0025	1114	4497	278482	3.33
3	24	8	8	1.4	2.45	0.66	54	3891	6	649	4658	571	78	0.88	0.1	1875	0.0101	0.0025	1055	3449	263800	3.01
3	24	8	8	1.6	2.29	0.65	47	3467	6	578	4365	516	62	0.89	0.1	1875	0.0082	0.0025	1006	2741	251573	2.76
3	24	8	8	1.8	2.16	0.63	42	3135	6	522	4123	472	50	0.90	0.1	1875	0.0067	0.0025	965	2238	241163	2.55
3	24	8	8	2.0	2.05	0.62	38	2868	6	478	3918	436	42	0.91	0.1	1875	0.0054	0.0025	929	1868	232143	2.37
5	24	8	4.8	0.2	3.46	0.81	625	38638	6	6440	31873	3963	2477	0.62	0.1	3125	0.0494	0.0078	2182	110089	545447	5.52
5	24	8	4.8	0.4	2.55	0.72	313	21190	6	3532	23725	2759	772	0.78	0.1	3125	0.0321	0.0045	1701	34323	425164	5.62
5	24	8	4.8	0.6	2.14	0.66	208	15121	6	2520	19662	2136	384	0.85	0.1	3125	0.0234	0.0028	1459	17074	364720	5.90
5	24	8	4.8	0.8	1.88	0.62	156	11987	6	1998	17161	1764	233	0.88	0.1	3125	0.0181	0.0025	1305	10372	326217	4.71
5	24	8	4.8	1.0	1.71	0.58	125	9810	6	1635	15053	1480	155	0.91	0.1	3125	0.0136	0.0025	1166	6869	291413	4.26
5	24	8	4.8	1.2	1.57	0.55	104	8175	6	1363	13231	1255	108	0.92	0.1	3125	0.0097	0.0025	1039	4799	259774	3.81
5	24	8	4.8	1.4	1.47	0.53	89	7007	6	1168	11835	1088	80	0.93	0.1	3125	0.0067	0.0025	940	3535	235001	3.52
5	24	8	4.8	1.6	1.39	0.51	78	6131	6	1022	10726	961	61	0.94	0.1	3125	0.005	0.0025	860	2709	214958	3.15
5	24	8	4.8	1.8	1.32	0.49	69	5450	6	908	9821	860	48	0.95	0.1	3125	0.005	0.0025	793	2138	198338	2.80
5	24	8	4.8	2.0	1.26	0.47	63	4905	6	818	9066	779	39	0.95	0.1	3125	0.005	0.0025	737	1729	184291	2.52
8	24	8	3	0.2	1.90	0.77	1000	64287	6	10715	88149	8199	2515	0.77	0.1	5000	0.0651	0.0110	2623	111786	655652	5.07
8	24	8	3	0.4	1.48	0.62	500	38443	6	6407	63718	5650	757	0.88	0.1	5000	0.0422	0.0066	1944	33645	486065	5.76
8	24	8	3	0.6	1.29	0.53	333	26160	6	4360	47449	4023	337	0.92	0.1	5000	0.0269	0.0039	1473	14961	368137	5.75
8	24	8	3	0.8	1.16	0.48	250	19620	6	3270	37634	3085	185	0.94	0.1	5000	0.0177	0.0025	1181	8229	295358	5.16
8	24	8	3	1.0	1.07	0.44	200	15696	6	2616	31307	2500	116	0.96	0.1	5000	0.0117	0.0025	991	5154	247764	4.77
8	24	8	3	1.2	1.01	0.41	167	13080	6	2180	26865	2101	79	0.96	0.1	5000	0.0075	0.0025	856	3508	213965	4.39
8	24	8	3	1.4	0.95	0.38	143	11211	6	1869	23563	1812	57	0.97	0.1	5000	0.005	0.0025	754	2530	188611	4.01
8	24	8	3	1.6	0.91	0.36	125	9810	6	1635	21005	1592	43	0.97	0.1	5000	0.005	0.0025	675	1904	168832	3.51
8	24	8	3	1.8	0.87	0.34	111	8720	6	1453	18963	1420	33	0.98	0.1	5000	0.005	0.0025	612	1480	152938	3.12
8	24	8	3	2.0	0.84	0.33	100	7848	6	1308	17292	1281	27	0.98	0.1	5000	0.005	0.0025	559	1181	139869	2.81
3	36	12	12	0.2	10.04	1.14	375	26325	6	4387	12181	2135	2253	0.49	0.15	2813	0.0513	0.0067	2204	100117	550931	6.03
3	36	12	12	0.4	7.11	1.13	188	13318	6	2220	9476	1476	744	0.66	0.15	2813	0.0340	0.0037	1877	33056	469129	6.04

Table A1 Continued

L_w (m)	H_w (m)	N_s	H_w/L_w	p (%)	αH	T_e (s)	A_f (m²)	V_b (kN)	R	V_b/R (kN)	M_w (kN-m)	V_w (kN)	V_f (kN)	V_w/V_b	P/P_o	P_o (kN)	ρ_b	ρ_{sh}	M_{beam} (kN-m)	K_{frame} (kN/m)	K_{beam} kN-m/rad	R_{exist}
3	36	12	12	0.6	5.81	1.11	125	8977	6	1496	7923	1119	377	0.75	0.15	2813	0.0241	0.0025	1670	16766	417472	4.96
3	36	12	12	0.8	5.04	1.10	94	6804	6	1134	6911	903	231	0.80	0.15	2813	0.0177	0.0025	1522	10260	380437	4.25
3	36	12	12	1.0	4.51	1.08	75	5498	6	916	6193	759	157	0.83	0.15	2813	0.0131	0.0025	1409	6982	352135	3.51
3	36	12	12	1.2	4.12	1.07	63	4627	6	771	5651	657	114	0.85	0.15	2813	0.0097	0.0025	1318	5089	329598	3.43
3	36	12	12	1.4	3.81	1.06	54	4004	6	667	5226	580	88	0.87	0.15	2813	0.0069	0.0025	1244	3890	311113	3.08
3	36	12	12	1.6	3.57	1.05	47	3536	6	589	4881	520	69	0.88	0.15	2813	0.005	0.0025	1182	3082	295605	2.78
3	36	12	12	1.8	3.36	1.03	42	3172	6	529	4595	472	56	0.89	0.15	2813	0.005	0.0025	1129	2508	282360	2.49
3	36	12	12	2.0	3.19	1.02	38	2880	6	480	4353	433	47	0.90	0.15	2813	0.005	0.0025	1084	2086	270882	2.26
5	36	12	7.2	0.2	5.39	1.24	625	41210	6	6868	36123	4076	2792	0.59	0.15	4688	0.0521	0.0081	2598	124093	649541	5.64
5	36	12	7.2	0.4	3.98	1.15	313	21921	6	3654	26687	2790	864	0.76	0.15	4688	0.0320	0.0046	2011	38395	502795	5.50
5	36	12	7.2	0.6	3.33	1.08	208	15280	6	2547	21913	2121	426	0.83	0.15	4688	0.0218	0.0028	1708	18921	426958	5.52
5	36	12	7.2	0.8	2.93	1.04	156	11885	6	1981	18974	1724	257	0.87	0.15	4688	0.0156	0.0025	1515	11403	378709	4.47
5	36	12	7.2	1.0	2.66	1.00	125	9813	6	1635	16952	1462	173	0.89	0.15	4688	0.0112	0.0025	1378	7691	344567	4.02
5	36	12	7.2	1.2	2.45	0.96	104	8410	6	1402	15458	1276	125	0.91	0.15	4688	0.0081	0.0025	1275	5574	318755	3.60
5	36	12	7.2	1.4	2.29	0.93	89	7394	6	1232	14300	1137	96	0.92	0.15	4688	0.0056	0.0025	1193	4246	298335	3.79
5	36	12	7.2	1.6	2.16	0.90	78	6623	6	1104	13369	1028	75	0.93	0.15	4688	0.005	0.0025	1127	3355	281637	3.34
5	36	12	7.2	1.8	2.05	0.88	69	6016	6	1003	12599	941	61	0.94	0.15	4688	0.005	0.0025	1071	2726	267635	3.03
5	36	12	7.2	2.0	1.96	0.86	63	5525	6	921	11950	870	51	0.94	0.15	4688	0.005	0.0025	1023	2265	255659	2.79
8	36	12	4.5	0.2	2.96	1.29	1000	63779	6	10630	97624	7918	2712	0.74	0.15	7500	0.0679	0.0105	3047	120515	761796	5.81
8	36	12	4.5	0.4	2.31	1.09	500	36615	6	6102	69481	5300	802	0.87	0.15	7500	0.0415	0.0060	2227	35664	556632	6.09
8	36	12	4.5	0.6	2.00	0.97	333	26727	6	4455	56578	4065	390	0.91	0.15	7500	0.0293	0.0039	1847	17315	461739	5.97
8	36	12	4.5	0.8	1.81	0.89	250	21481	6	3580	48847	3347	233	0.93	0.15	7500	0.0221	0.0027	1616	10352	403875	5.31
8	36	12	4.5	1.0	1.67	0.83	200	18184	6	3031	43566	2874	156	0.95	0.15	7500	0.0171	0.0025	1455	6944	363729	4.83
8	36	12	4.5	1.2	1.57	0.78	167	15899	6	2650	39668	2537	113	0.96	0.15	7500	0.0134	0.0025	1335	5010	333695	4.78
8	36	12	4.5	1.4	1.48	0.74	143	14211	6	2368	36638	2283	86	0.96	0.15	7500	0.0106	0.0025	1240	3801	310084	4.41
8	36	12	4.5	1.6	1.41	0.71	125	12906	6	2151	34194	2084	67	0.97	0.15	7500	0.0083	0.0025	1163	2992	290862	4.19
8	36	12	4.5	1.8	1.36	0.68	111	11864	6	1977	32169	1923	55	0.97	0.15	7500	0.0064	0.0025	1099	2423	274800	3.86
8	36	12	4.5	2.0	1.31	0.65	100	11009	6	1835	30455	1790	45	0.98	0.15	7500	0.005	0.0025	1044	2006	261106	3.71

L_w=wall length; H_w=wall height; N_s=number of stories; H_w/L_w=aspect ratio of wall; p=wall index; aH=behavior factor; T_e=elastic period of structure; A_f=floor area per wall; V_b=unfactored total equivalent seismic base shear; R=force reduction factor; M_w=wall design bending moment; V_w=wall base shear; V_f=frame base shear; P_o=axial load; r_b=ratio of total boundary element longitudinal reinforcement area to boundary region area; r_{sh}=web reinforcement; M_{beam}=total bending effect of beams framing to walls; K=initial stiffness of beam and frame elements